Research Article

Extraction and characterization of cellulose from halophytes: next generation source of cellulose fibre

Aneesha Singh[1] · **Bablesh Ranawat**[1] · **Ramavatar Meena**[2]

Abstract

Cellulose content was estimated from *Tamarix aphylla*, *Juncus rigidus*, and *Thespesia populnea* growing in saline soil at salt farm experimental plot of Central Salt and Marine Chemicals Research Institute (CSMCRI), Bhavnagar, Gujarat, India. Cellulose was extracted from the plant samples by the treatment of $NaClO_2$ followed by NaOH, HCl, and H_2O_2. Extracted cellulose samples were fractionated to α-cellulose and β-cellulose. *Tamarix aphylla* was subject to different treatments, and among all the treatments the highest cellulose fibre was extracted from T1 (3.0% $NaClO_2$ followed by 17.5% NaOH, 4.0% HCl) with 33% α-cellulose having 61% crystallinity. Maximum (44.0%) crude cellulose (3.5% $NaClO_2$ followed by 2.0% NaOH, 5.0% HCl, 17.5% NaOH) was obtained from J2 treatment (*J. rigidus*) with 58.7% crystallinity, 33% α-cellulose with 62% crystallinity and TP3 (4.0% $NaClO_2$ followed by 4.0% NaOH, 5.5% HCl, 17.5% NaOH) was best for *T. populnea* with 39% highest crude cellulose with 64.4% crystallinity, 30% α-cellulose with 55% crystallinity. The cellulose related peaks were noted in XRD and FTIR spectra; lignin and hemicellulose related peaks were absent. This confirms the removal of lignin and hemicellulose from the isolated product. All the three halophytes growing in saline soil were found good source of cellulose. However, *T. aphylla* contain highest cellulose and α-cellulose with highest crystallinity as compared to *J. rigidus,* and *T. populnea*.

Keywords Halophyte · *Juncus rigidus* · Salinity · *Tamarix aphylla* · *Thespesia populnea*

1 Introduction

There is immense use of paper in day to day life, paper is natural cellulose fibre and till today there is no green substitute of it. Plants are major contributors of natural cellulose. High demand of paper has generated great impact on deforestation and around 40% annually wood is harvested for making paper and paperboard. With the continuously increasing demand of paper in the last 40 years, the paper consumption growth has reached 400%. Around 4 billion trees are cut in the world for paper making. Today, the world consumption of paper is about 300 million tons per year. About, 38% of the world's total fibre supply is fulfilled by virgin pulp, and recycled paper. Major contributors in paper making are wood fibre plants and followed by non-wood fibre plant (grass, cotton, flax, hemp, jute, ramie, kenaf, bamboo, baggage, cereal straw) contributors [35–37]. Major cellulose plant contributors grow on cultivable land. In India, nearly 9.38 million hector lands is salt-affected, 5.5 million hectors land is saline that includes coastal land and alkali land of about 3.88 million hector [19]. Due to edaphic factors agricultural land is also converting into saline land and causing depletion of fertile land; coastal and arid areas are under prone zones. Hence, there is need to use saline wasteland to complete future demands of increasing population. Looking the current scenario, it has become very essential to resolve this issue by identifying crops which can grow on wasteland without compromising end product. Halophytes are salt loving plants and grow on high TDS soil. *Tamarix aphylla,*

✉ Aneesha Singh, aneesha.singh@rediffmail.com; aneeshas@csmcri.res.in | [1]Division of Biotechnology and Phycology, Central Salt and Marine Chemicals Research Institute (Council of Scientific and Industrial Research), G.B Marg, Bhavnagar, Gujarat 364002, India. [2]Natural Products and Green Chemistry Division, Central Salt and Marine Chemicals Research Institute (Council of Scientific and Industrial Research), G.B Marg, Bhavnagar, Gujarat 364002, India.

SN Applied Sciences (2019) 1:1311 | https://doi.org/10.1007/s42452-019-1160-6

Received: 12 April 2019 / Accepted: 23 August 2019 / Published online: 1 October 2019

Juncus rigidus, and *Thespesia populnea* are the halophytes that can tolerate high salinity, aridity [62]. They are found inland and by the sea in saline habitats.

Tamarix aphylla L. Karst belongs to family Tamaricaceae. Plant height reaches up to 18 m., known as Athel tamarisk, and Saltcedar. *Tamarix aphylla* wood is used for fuel, particle boards and cellulose [64]. *Tamarix sp.* can grow in arid and semi-arid climates, and may bear variations in soil dampness, if groundwater is available [14]. The plants possess proline analogues that help in adopting the adverse effects of sodium chloride [53]. *Tamarix* is fast growing plant, 2400 trees/ha may generate biomass 25 ton/ha/year with saline water irrigation [12].

Thespesia populnea (L.) Sol. ex Correa a multipurpose tree, the leaf extracts can be used by diabetics [18, 48], other plant parts are key ingredient of several ayurvedic preparations namely "panchvalkala" lepa, abhyanga, and parisheka [56]. Bark is a good source of fabric dye [16]. *Thespesia populnea* has been extensively studied for its pharmacological, antioxidant, antimicrobial and medicinal values [29, 33, 42, 63]. Also, it is potential candidate for biodiesel as its biodiesel specifications are comparable with ASTM D6751 and EN 14214 [43, 44]. Cellulose of *Thespesia lampas* has been studies for its structural and physical properties [5, 45]. *Thespesia populnea* being potential source material for cellulose, it has not been well studied.

Juncus rigidus L. known as sea rush and commonly seen in the marsh and saline areas. It reclaims degraded saline soil by decreasing soil TDS [3, 59]. *Juncus* clums are used for making good quality mats [61]. The use of *Juncus* sp culms for paper industry is well documented [8, 62]. It is considered a potential plant of the raw material of paper industry [60, 62]. It was estimated that one ton dry biomass of *Juncus* might produce 375–400 kg pulp [60]. *Juncus acutus* L. has been studied for cellulosic fibre [4], however no such studies are available for *J. rigidus.*

To best of our knowledge, this is first report on optimization of cellulose extraction method, profiling, and characterization. In the present study, the cellulose extraction method is optimised using different concentrations of acid, alkaline solution and bleaching agent at different temperature. The cellulose was characterised using SEM, XRD, FTIR NMR and TGA. It was known by the study that these three parameters plays significant role on quantity of extracted cellulose of *T. aphylla, J. rigidus* and *T. populnea*.

2 Materials and methods

Cellulose was isolated from the halophytes as described by per Mihranyan et al. [32]. Plant material of 1.5 inch diameter was collected from 3 years old plants growing in salt farm area, Central Salt and Marine Chemicals Research Institute, Bhavnagar, Gujarat, India (latitude 21°47.3060 N and longitude 72°7.4170 E). The plant materials were oven dried (80 °C) and cut in pieces, further crushed by mixer. The crushed plant materials were bleached by treating with $NaClO_2$ (36 g $NaClO_2$ was added to 1 L acetate buffer) at 100 °C for 3–6 h (Fig. 1). The bleached plant materials pH were neutralized by washing with water until reaches 7 pH. The washed materials were treated with 2–17.5% NaOH solution and heated at 100 °C (Fig. 1). The NaOH treated plant materials were washed until pH is neutralized 7pH. The filtered material was dried at room temperature. The dried material was again treated with 2–4% (v/v) hydrochloric acid and was heated up to 100 °C for different hrs (Fig. 1). The product was washed by water to remove the acid, filtered, air dried and oven dried at 50 °C before taking dry weight of cellulose. Cellulose yield was calculated on the basis of plant dry weight.

The α-cellulose and β-cellulose fractionated from cellulose as per method published by Whistler [57]. One gram oven dried cellulose was treated with 17.5% NaOH (w/v) solution and heated at 100 °C for 4 h. The slurry was filtered, β-cellulose was collected as supernatant, and α-cellulose was obtained after frequent washing with water up until 7 pH was obtained. The product was air dried and followed by oven drying at 50 °C for 6 h. 3 N H_2SO_4 (20 ml) was added to the supernatant to precipitate β-cellulose, and heated at 80 °C for 10 min. The precipitated solution was centrifuged and β-cellulose was collected. β-cellulose was washed by water until pH 7. The cellulose was air dried and followed by oven drying at 50 °C for 6 h. The yield was determined using three replicates. The samples were finely powered and studied using Philips X'pert MPD X-ray powder diffractometer. The relative crystallinity index (CI) was calculated by Mihranyan et al. [32] method, $CI\ (\%) = ([(I_{002} - I_{am})]/I_{002}) \times 100$. I_{002} and I_{am} were the intensity corresponding to the peak at $2\theta = 22°$ and $2\theta = 18°$, respectively. The apparent crystallite size was estimated through the use of the Scherrer equation [50]: $L = (K \times \lambda)/(\beta \times \cos\theta)$. Where K is 0.94 constant, λ is the X-ray wavelength (0.1542 nm for Cu Ka radiation), β is the half-height width of diffraction band and θ is the Bragg angle corresponding to the (002) plane. The proportion of crystallite interior chains [10] is: $X = (L - 2h)^2/L^2$. Where L is the crystallite size to the (002) plane, h = 0.57 nm is the thickness of the layer of surface chain.

The FTIR spectra of all the cellulose samples were performed to study the effect of alkali, acid and bleaching treatments on cellulose. The IR spectra were studied on a Perkin–Elmer Spectrum GX FTIR (USA) instrument to identify the constituents of isolated fibres. IR spectra were noted in a transmittance mode and scanning range was 500–4000 cm^{-1}. The degree of crystallinity was calculate by Schenzel et al. [49]; $\%X_c^{\ RAMAN} = I_{1481}/I_{1481} + I_{1462}$.

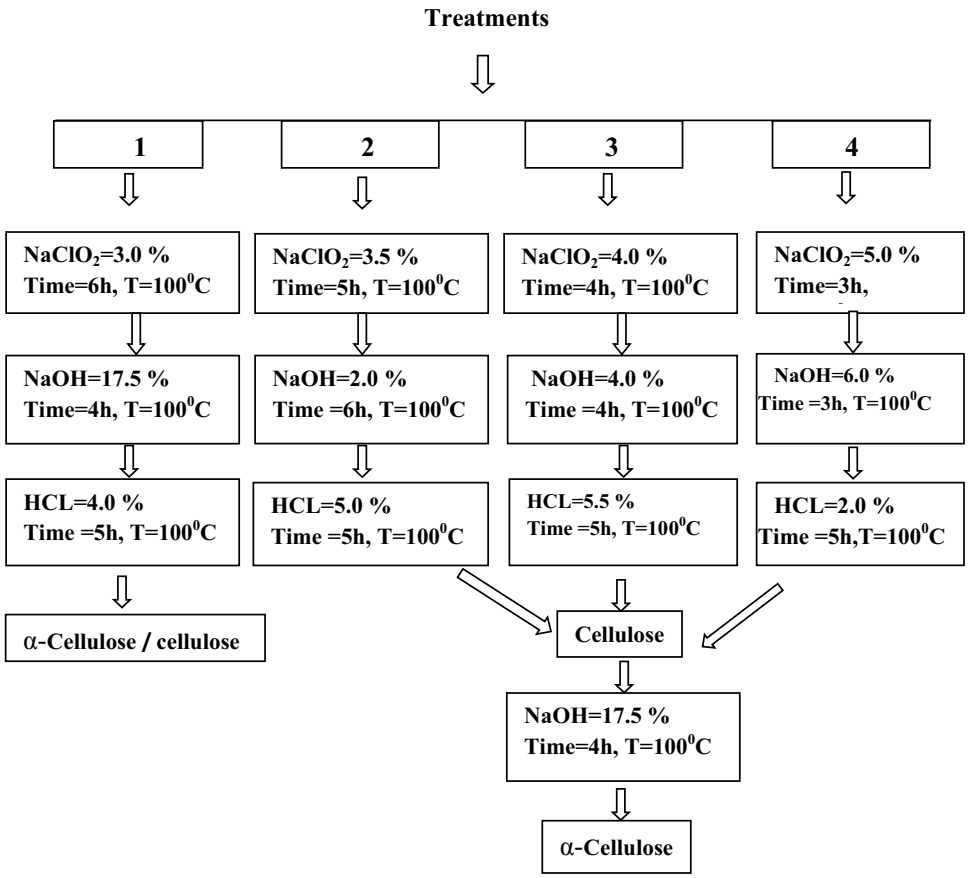

Fig. 1 Schematic diagram for the isolation of cellulose from halophytes

Here I_{1462} and I_{1481} are the Raman intensities at 1462 cm^{-1} (amorphous) and 1481 cm^{-1} (crystalline), respectively. The characterization of cellulose, and α-celluloses of halophyte was carried by solid state NMR (CP-MAS ^{13}C NMR) measurements at 20 °C on a Brüker Avance 500 MHz, Spectrometer (Switzerland) at 52.3 MAS, net spinning was kept at 5000 rpm/min. Cellulose morphology was studied using Scanning Electron Microscopy (SEM) (model Philips XL 30). Thermogravimetric analysis **(**TGA) was performed on Thermal Gravimetric Analyzer, Mettler Toledo and Netzsch TG 209 F1. The samples were heated from 50 to 800 °C at the rate of 20 °C/min under nitrogen flow. 2–3 mg samples were used in an aluminium pan under nitrogen atmosphere.

3 Results and discussion

The X-ray diffraction (XRD) is used for estimating the degree of crystallinity. The rigidity and flexibility of the cellulose fibre depends on crystalline and amorphous ratio [15]. Cellulose is crystalline, although hemicellulose and lignin are amorphous [21]. Cellulose is composed of two crystalline structure α-cellulose and β-cellulose. Cellulose is triclinic and α-cellulose and β-cellulose are monoclinic unit cells [39]. The plant samples were subject to different treatments as per Fig. 1 for optimizing cellulose extraction method. Among, all the treatments (T1, T2, T3 and T4) the highest yield of α-cellulose (36.6%) with 61.8% crystallinity Index (CI) and 7.3% β-cellulose was obtained from *T. aphylla,* T1 treatment. J2 was best treatment for *J. rigidus* with highest yield of 44% crude cellulose with 58.7% crystallinity, 33% α-cellulose with 54% crystallinity and 8.6% β-cellulose (Figs. 2, 3, 4). TP3 was best for *T. populnea* with maximum yield of 39.3% crude cellulose with 64.5% crystallinity, 32.2% α-cellulose with 48% crystallinity and 7.7% β-cellulose (Figs. 2, 3, 4).

3.1 X-ray diffraction

The XRD profile of all the crude cellulose samples developed diffraction peaks of type I cellulose (Fig. 5a). The XRD profile of J2 crude cellulose developed well define crystalline peaks around 2θ were 16.0°, 22.6° and 34.9°; TP3 were 16.1°, 22.5°, and 34.7° corresponding to the (101), (10$\bar{1}$) (002) and (040) crystallographic planes of cellulose type I, respectively (Fig. 5b). Crystallographic planes are labelled as per the cellulose I structure described by Segal et al. [51]. These peaks represents type I cellulose [21, 38]. T1 developed diffraction peaks at 2θ around 12.29°, 20.5°,

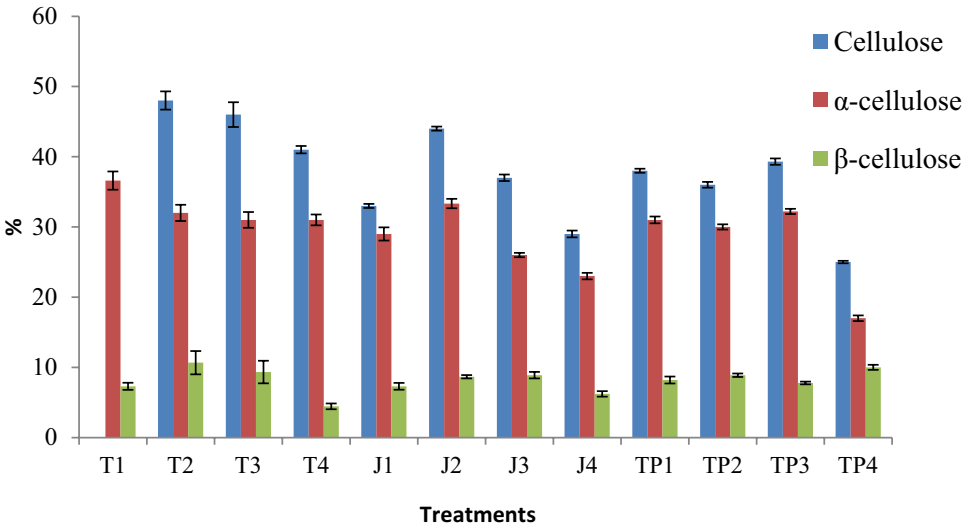

Fig. 2 Yield (%) of crude cellulose, α-cellulose and β-cellulose obtained from halophytes; T1-*Tamarix aphylla,* TP3-*Thespesia populnea*, J2-*Juncus rigidus* samples. n = 3

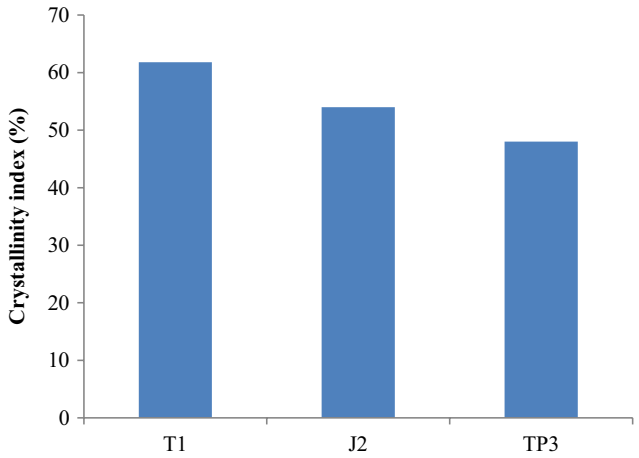

Fig. 3 The percent crystallinity index of α-cellulose of T1-*Tamarix aphylla,* TP3-*Thespesia populnea*, J2-*Juncus rigidus*

22.28°, and 34.9° corresponding to the (101), (10$\bar{1}$), (002) and (040) crystallographic planes of α-cellulose, respectively (Fig. 5b). These peaks reported as of α-cellulose [30].

3.2 FT-IR spectroscopy

For *T. aphylla* (T1), 20% NaOH treatment was optimum for the extraction of α-cellulose. However, the same treatment was unable to extract α-cellulose from other two halophytes (*J. rigidus*, *T. populnea*). *J. rigidus* (J2) and *T. populnea* (TP3) were further alkaline hydrolysed with 17.5 M NaOH for the extraction of α-cellulose. J2 α-cellulose diffraction peaks at 2θ were 12.29°, 20.20°, and 22.90°; TP3 at 12.31°, 20.21, and 22.36° (Table 1). The *d*-spacing of TP3, J2 and T1 cellulose samples were obtained from XRD profiles was 3.9 Å (Table 1). The crystallite size of (002) plane for TP3, J2

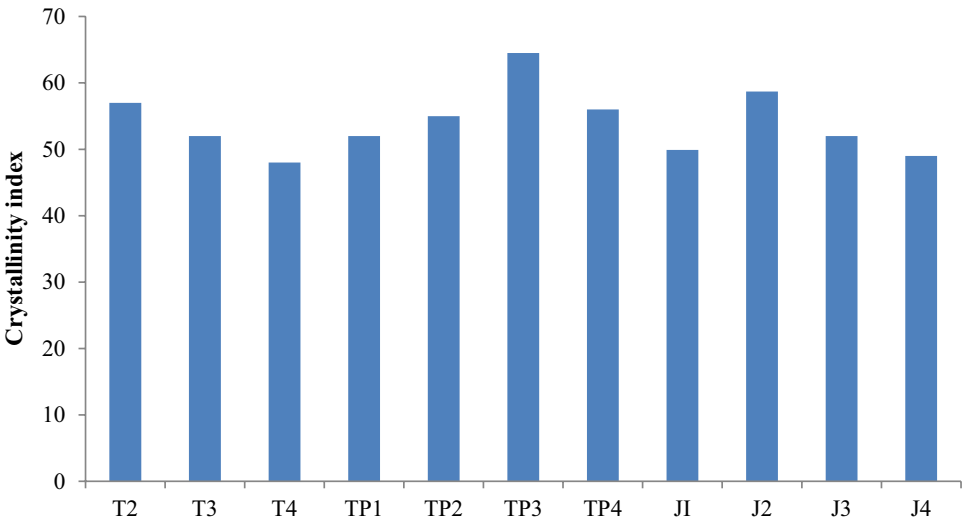

Fig. 4 The crystallinity index of crude cellulose obtained from all the samples of halophytes

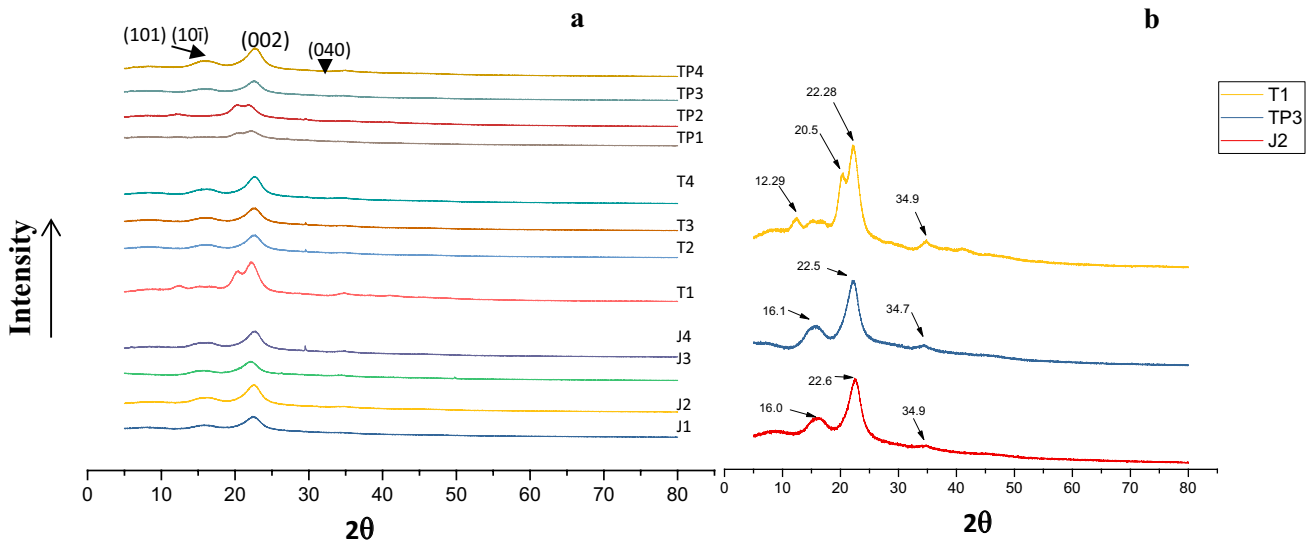

Fig. 5 XRD profile of crude cellulose obtained from halophytes (**a**), XRD 2θ peak values for cellulose of T1, TP3 and J2 samples (**b**)

Table 1 XRD 2θ peak values, crystallinity index, *d*-spacing, apparent crystallite size and proportion of crystallite interior chains of α-cellulose for the studied samples

Samples	2θ peaks	Crystallinity index CI (%)	*d*-spacing (Å)	Crystallite size L002 (nm)	Proportion of crystallite interior chains X
TP3	20.2161				
	22.3618	48	3.9	4.1	0.5
	12.3101				
J2	20.2019				
	22.9024	54	3.9	2.9	0.3
	12.2901				
T1	20.5121				
	22.2801	61.8	3.9	1.8	0.1
	12.2923				

TP3-*Thespesia populnea*, J2-*Juncus rigidus*, T1-*Tamarix aphylla*

and T1 samples were different may be because of different treatment applied to them for achieving optimum cellulose. The proportion of crystallite interior chains reduces with the reduction of crystallite size of the plane (002). The results were corroborating Sugar cane bagasse XRD study [9]. TP3 crystallite size was highest among all the samples (Table 1).

The Fourier Transform Infrared (FTIR) spectroscopy is a useful technique for studying the structural changes occurred by the various treatments in the isolated cellulose. The FTIR spectra of all the three α-cellulose samples (T1, J2, and TP3) of halophytes were identical. Crystallinity of J2 cellulose was highest (51.48%) among all the samples; the crystallinity was calculated by comparing the intensity peaks from FTIR spectra (Fig. 6). A broad band region of 3700–3000 cm^{-1} was assigned to hydrogen bonded (O–H) stretching and other region 3000–2800 cm^{-1} was

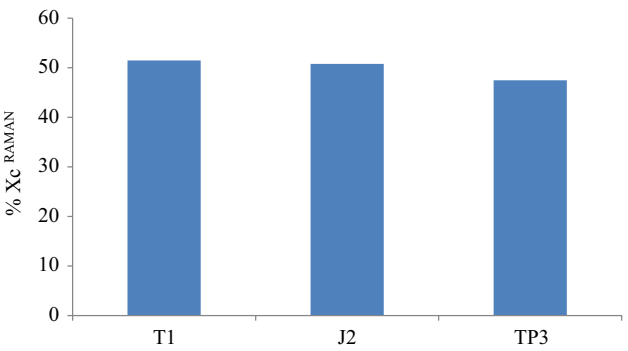

Fig. 6 Calculated values of crystallinity of cellulose by comparing the intensity peaks from FTIR spectra

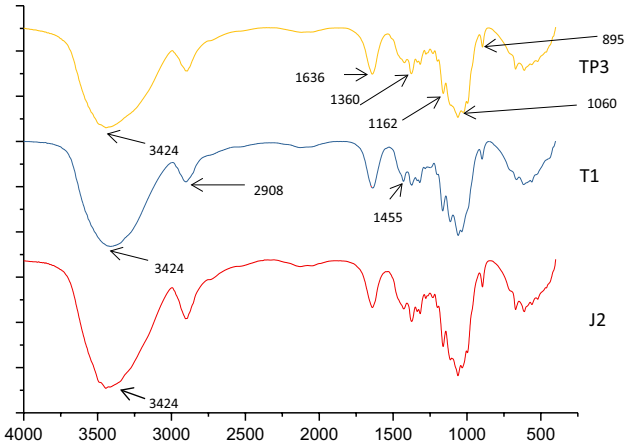

Fig. 7 FTIR spectra of alpha cellulose of T1, TP3 and J2 samples

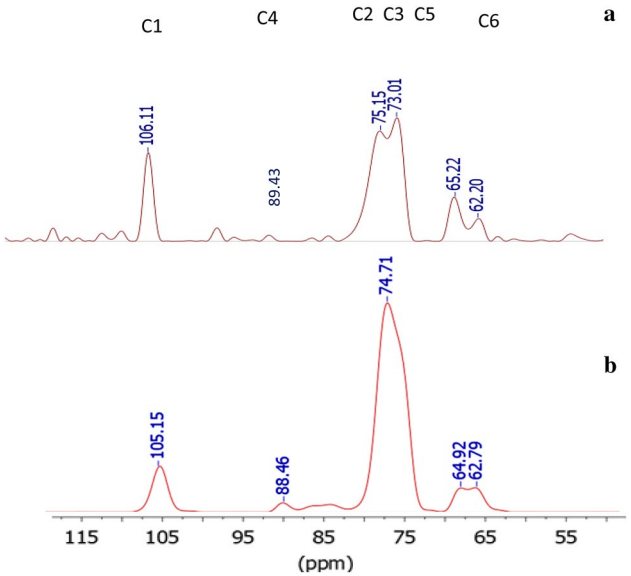

Fig. 8 CP/MAS 13C NMR spectra of cellulose: **a** cellulose of halophyte; **b** α-cellulose of halophyte

assign to asymmetric, symmetric methyl and methylene CH cellulose group [17, 41]. All samples developed broad peak at 3424 cm^{-1} are ascribed to O–H stretching assign for water (Fig. 7). The broad band region 2908 cm^{-1} is of C–H stretching vibration assign to cellulose component [17, 20]. The band at 1636 cm^{-1} is associated with absorbed water in cellulose (Fig. 7). The 1455 cm^{-1} band is ascribed to CH_2, CH_3 symmetric bending in cellulose [11]. 1360 cm^{-1} are ascribed to CH group in a glucose unit [2]. In the present study, the bands at 1162 cm^{-1} are attributed to C–O–C bridge stretching at the β(1,4)-glycosidic linkage, 1060 cm^{-1} ascribed to C–OH stretching vibration of the cellulose back bone, 895 cm^{-1} assign to β-glycosidic linkage [2, 6, 11, 65], all these band were observed in all the samples (Fig. 7). The band 1731 cm^{-1} ascribed to the carbonyl stretching vibration of hemicellulose [1] was absent in all the three samples. Also, IR spectra peaks at 1269 cm^{-1} ascribed to C=O stretching vibration of lignin, aromatic skeletal vibration of lignin 1510 cm^{-1} and 1596 cm^{-1} bands [13] were absent in the present study. Lignin and hemicellulose related peaks were also absent or minimised significantly. This result reveals the removal of lignin and hemicellulose from all samples and peaks related to cellulose structural change were also not observed. It was known by the Raman spectra analysis that extracted cellulose was rich in cellulose I_α.

3.3 NMR spectroscopy

The CP-MAS ^{13}C-NMR spectra gives us the carbon backbone of a molecule, the ^{13}C NMR spectral values of halophyte cellulose were corroborating with the previous reports of ^{13}C NMR of cellulose [34, 52, 55, 58]. The spectra of crude cellulose of halophyte developed doublet between 72 and 82 ppm (Fig. 8). Chemical shift values of α-cellulose of halophyte developed a single broad peak between 72 and 82 ppm (Fig. 8) may be because of the superimposing resonances of C-2, C-3 and C-5 carbons [24].

The values of chemical shifts between 60 and 67.5 ppm of C-6, and the chemical shift value of C-4 and C-1 carbons of halophyte were also similar and comparable with the previous reports on cellulose [24, 54]. Signals at 55 ppm, 115 ppm, and 126 ppm were absent in Fig. 8, these peaks are exclusively for lignin [27, 28, 46]. While the peaks 64.92, 62.79, 74.71, 88.46, 105.15 coincide with cellulose peaks [27, 28]. The absence of most of the hemicelluloses peaks 102, 107, 159, 168 (Fig. 8b) implies that the hemicellulose components were successfully removed from the isolated α-cellulose.

Figure 9 shows the SEM images of untreated (a, c) and treated cellulose with 17% NaOH (b, d, e), the untreated fibres are bounded with each other while the treated once are free. It was clear from the Fig. 8 that all the remaining impurities were removed from the cellulose by the treatment of NaOH.

3.4 Thermal stability analysis

It is important to determine the pyrolysis of natural fibre at high temperature before it is used as composite polymer. Also, the thermal degradation of natural fibres needs to be studied to avoid degradation during the manufacturing process. TGA performed samples showed the percent weight loss as a function of temperature. In the first step water loss was observed in all the three samples around 100 °C, and further thermal degradation took place as

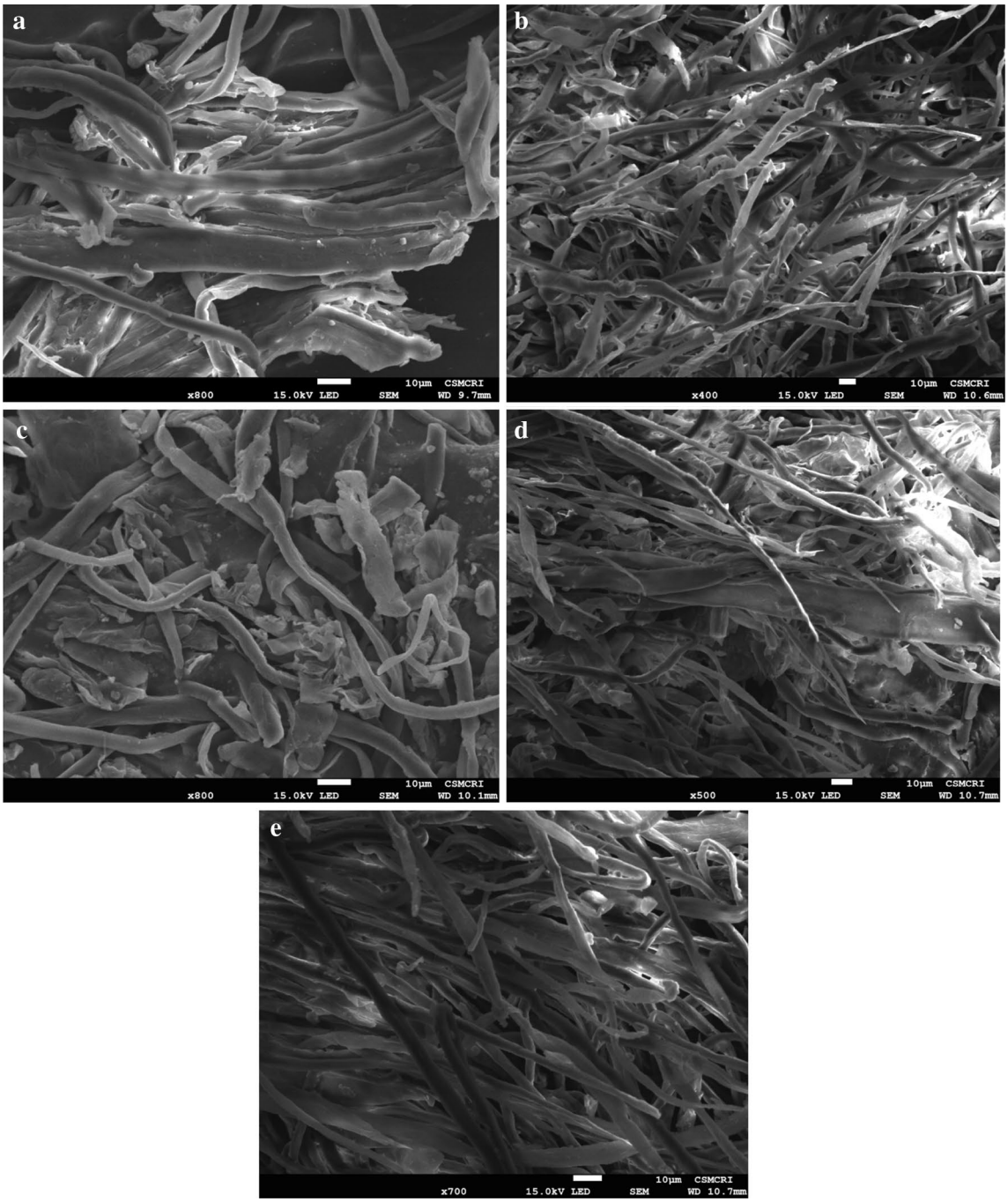

Fig. 9 Cellulose of *Thespesia populnea* (**a**) *Thespesia populnea* cellulose treated with 17% NaOH (**b**), Cellulose of *Juncus rigidus* (**c**) *Juncus rigidus* cellulose treated with 17% NaOH (**d**) *Tamarix aphylla* cellulose treated with 17% NaOH (**e**)

three-step process (Fig. 10). Pyrolysis at 100–230 °C may be considered as second step. In this duration weight of the samples was almost constant of all the samples; it implies that all the samples were thermally stable at 212–230 °C (Fig. 10). In third step, TP3 sample initiates distinct degradation process at around 238 °C (onset) to 387 °C (end set). The pyrolysis around 336 °C is assigned to cellulose and lignin decomposition [31]. The random cleavage of the glycosidic linkage of cellulose occurs at this stage [40]. For TP3 sample, 78.4% weight loss noted between 238 to 387 °C. The higher onset of pyrolysis indicates more thermal stability of TP3 as compared to other samples. More number of H bonds between cellulose chains and their arrangement may be responsible for high thermal stability [47]. The crystallite size of TP3 was larger than other two samples. The higher crystallite size celluloses have higher

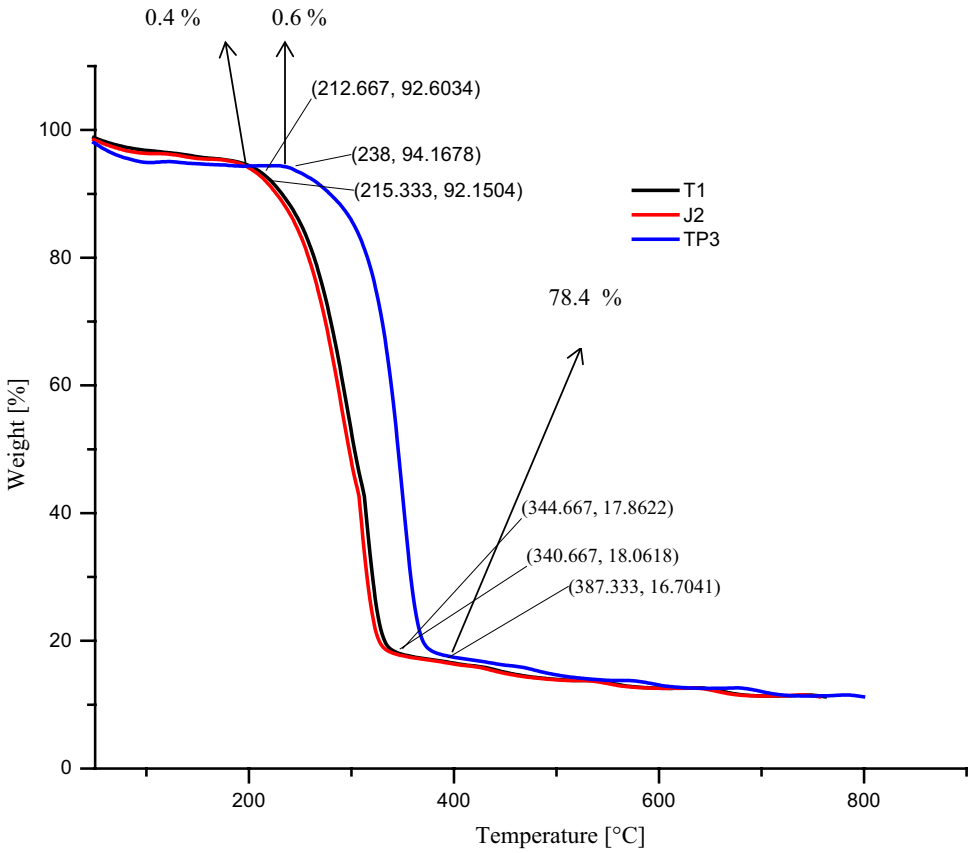

Fig. 10 TGA curves of TP3, T1 and J2 cellulose

thermal stability [23]. The fourth step decomposition starts around 387 °C assigned to cellulose and lignin decomposition. For T1 and J2 samples major degradation (78%) process occurs at 212–340 °C and 215–344 °C respectively. The thermal stability of T1 and J2 were comparatively less than TP3.

The halophytes crude cellulose yield was in range of 39–48%. However, the other woody plant reported to have 38% of crude cellulose [26] and 41.5% of crude cellulose from *Eucalyptus* [22, 26]. The 34.2% crude cellulose was obtained from *Pine radiata* [7]. Bamboo and teak possessed 43% and 44% crude cellulose, respectively (Singh et al. unpublished data). Teak wood reported to have 40–49% crude cellulose [25]. It was known by the study that the cellulosic content of *T. aphylla*, *T. aphylla* and *J. rigidus* were comparable with other plants [7, 26]. The results reveal that *T. aphylla* requires comparative low concentration of $NaClO_2$, HCl and more heating time for the removal of lignin and hemicellulose than other halophytes. The α-cellulose isolated from *T. aphylla* showed the highest percent crystallinity index (C.I. = 61.8%), while the lowest (C.I. = 48%) was noted from *T. populnea*.

This study has given an overall trend on the cellulose profile of some Indian halophytes. Cellulose extraction method was optimized for all the three halophytes. The highest α-cellulose was obtained from *T. aphylla* and lowest was from *T. populnea*. More number of halophytes may be considered, however, some of the halophytes explored here can be of use as source of cellulose for industrial applications.

Acknowledgements CSIR-CSMCRI Communication No. CSIR-CSMCRI-023/2019. The financial support received from CSIR, New Delhi, India (Project OLP0067) is thankfully acknowledged.

Funding The financial support received from CSIR, New Delhi, India (Project OLP0067).

Compliance with ethical standards

Conflict of interest The authors declare that they have no conflict of interest.

Human and animal rights Research involving no human participants and/or animals. The manuscript is processed through proper channel.

References

1. Abraham E, Deepa B, Pothan LA, Jacob M, Thomas S, Cvelbar U, Anandjiwal R (2011) Extraction of nanocellulose fibrils

from lignocellulosic fibres: a novel approach. Carbohy Poly 86:1468–1475
2. Adel AM, Abd El-Wahab ZH, Ibrahim AA, Al-Shemy MT (2010) Characterization of microcrystalline cellulose prepared from lignocellulosic materials. Part I. Acid catalyzed hydrolysis. Bioresour Technol 101:4446–4455
3. Alshammary SF (2007) Some potential plant of coastal and inland salt affected soil and there relation to soil properties. Asian J Plant Sci 6:821–826
4. Amel EG, Marzoug IB, Hassen MVB, Roudesli MS (2012) Separation and characterization of new cellulosic fibres from the *Juncus acutus* L. plant. Bioresources 7:2002–2018
5. Ashok B, Reddy KO, Madhukar K, Cai J, Zhang L, Rajulu AV (2015) Properties of cellulose/*Thespesia lampas* short fibers bio-composite films. Carbohy Poly 127:110–115
6. Bessadok A, Marais S, Roudesli S, Lixon C, Métayer M (2008) Influence of chemical modifications on water-sorption and mechanical properties of Agave fibres. Compos Part A 39:29–45
7. Borella SML, Saurer M, Siegwolf R (1998) Reducing the uncertainties in d13C analysis of tree rings: pooling, milling, and cellulose extraction. J Geophys Res 103:19519–19526
8. Boyko H (1966) Basic ecological principles of plants growing by irrigation with highly saline or sea water. In: Hoyko H (ed) Salinity and aridity. Dr. W. Junk Publishers, The Hague, pp 131–200
9. Chen MJ, Zhang XQ, Matharu A, Melo E, Li RM, Liu CF, Shi QS (2017) Monitoring the crystalline structure of sugar cane bagasse in aqueous ionic liquids. ACS Sustain Chem Eng 5:7278–7283
10. Davidson TC, Newman RH, Ryan MJ (2004) Variations in the fibre repeat between samples of cellulose I from different sources. Carbohydr Res 339:2889–2893
11. De Rosa IM, Kenny JM, Puglia D, Santulli C, Sarasini F (2010) Morphological, thermal and mechanical characterization of okra (*Abelmoschus esculentus*) fibres as potential reinforcement in polymer composites. Compos Sci Tech 70:116–122
12. Eshel A, Zilberstein A, Alekparov C, Eilam T, Oren I, Sasson Y, Valentini R, Waisel Y (2014) Biomass production by desert halophytes: alleviating the pressure on food production. In: Rosen MA, Perryman R, Dodds S, Mizi F, Yuji W, Polkowsaka Z, Sobik M (eds) Recent advances in energy & environment: proceedings of the 5th IASME/WSEAS international conference on energy & environment (EE'10). WSEAS Press, Stevens Point, WI, pp 362–367
13. Faix O (1992) Fourier transform infrared spectroscopy. In: Lin SY, Dence CW (eds) Methods in lignin chemistry. Springer Series in Wood Science. Springer, Berlin, pp 233–241
14. Frasier GW, Johnsen TN (1991) Saltcedar (tamarisk). In: James LF, Evans JO, Ralphs MH, Child RD (eds) Classification, distribution, ecology and control in noxious range weeds. Westview Press, Boulder, pp 377–386
15. Gümüskaya E, Usta M, Kirei H (2003) The effects of various pulping conditions on crystalline structure of cellulose in cotton linters. Polym Degrad Stab 81:559–564
16. Gunturu B, Rao PN, Renganathan S (2018) Decolorisation of basic textile dye from aqueous Solutions using a Biosorbent derived from *Thespesia populnea* used Biomass. In: IOP conference series: materials science and engineering, p 330 012036
17. Guo X, Liu L, Wu J, Fanb J, Wu Y (2018) Qualitatively and quantitatively characterizing water adsorption of a cellulose nanofiber film using micro-FTIR spectroscopy. RSC Adv 8:4214–4220
18. Haja SS, Moideen K, Sengottuvelu S, Sivakumar T (2011) Antidiabetic effect of methanolic extract of *Thespesia populnea* flower and leaf in normal and alloxan-induced diabetic rats. Int J Res Ayurveda Pharm 2:936–939
19. IAB (2000) Indian agriculture in brief, 27th edn, Agriculture Statistics Division, Ministry of Agriculture, Govt. of India, New Delhi
20. Jayaramudu J, Guduri BR, Varada Rajulu A (2010) Characterization of new natural cellulosic fabric Grewia tilifolia. Carbohy Poly 79:847–851
21. Johar N, Ahmada I, Dufresne A (2012) Extraction, preparation and characterization of cellulose fibres and nanocrystals from rice husk. Ind Crop Prod 37:93–99
22. Kasmani JE, Nemati M, Samariha A, Chitsazi H, Mohammadi NS, Nosrati H (2011) Studying the effect of the age in *Eucalyptus camaldulensis* species on wood chemical compounds used in pulping process American-Eurasian. J Agric Environ Sci 11:854–856
23. Kim UJ, Eom SH, Wada M (2010) Thermal decomposition of native cellulose: influence on crystallite size. Polym Degrad Stab 95:778–781
24. Kono H, Yunoki S, Shikano T, Fujiwara M, Erata T, Takai M (2002) CP/MAS 13C NMR study of cellulose and cellulose derivatives. 1. Complete assignment of the CP/MAS 13C NMR spectrum of the native cellulose. J Am Chem Soc 124:750–751
25. Lukmandu G (2015) Termites and teak composition. Bioresource 10:20194–22102
26. Macfarlane C, Warren CR, White DA, Adams MA (1999) A rapid and simple method for processing wood to crude cellulose for analysis of stable carbon isotopes in tree rings. Tree Physiol 19:831–835
27. Martinez AT, Gonzalez AE, Valmaseda M, Dale BE, Lambregts MJ, Haw JF (1991) Solid-state NMR-studies of lignin and plant polysaccharide degradation by fungi. Holzforschung 45:49–54
28. Martinez AT, Almendros G, Gonzalez-Vila FJ, Frund R (1999) Solid-state spectroscopic analysis of lignins from several Austral hardwoods. Solid State Nucl Magn Reson 15:41–48
29. Marwat SK, Fazal-Ur-Rehman MAK, Ahmad M, Zafar M, Ghulam S (2011) Medicinal folk recipes used as traditional phytotherapies in district Dera Ismail Khan, KPK, Pakistan. Pak J Bot 43:1453–1462
30. Mat Soom R, Aziz AA, Wan Hasan WH, Mat Top ABG (2009) Solid state characteristics of microcrystall cellulose from oil palm empty fruit bunches Fibre. J Oil Palm Res 21:613–620
31. McNeill I, Memetea L, Cole W (1995) A study of the product of PVC thermal degradation. Polym Degrad Stab 49:181
32. Mihranyan A, Llagostera AP, Karmhag R, Strømme M, Ek R (2004) Moisture sorption by cellulose powders of varying crystallinity. Int J Pharm 269:433–442
33. Mohammedi Z, Atik F (2011) Impact of solvent extraction type on total polyphenols content and biological activity from *Tamarix aphylla* (L.) karst. Int J Pharm BioSci 2:609–615
34. Nascimentoa P, Marima R, Carvalhob G, Malia S (2016) Nanocellulose produced from rice hulls and its effect on the properties of biodegradable starch films. Mater Res 19:167–174
35. Omar K, Lwako M, Joseph KB, Baptist KJ (2013) A review on pulp manufacture from non wood plant materials. Int J Chem Eng Appl 4:144–148
36. Pahkala KA, Paavilainen L, Mela T (1997) Grass species as raw material for pulp and paper. In: Proceedings XVIII IGC (internatioal grassland congress) 1997 Winnepeg, Manitoba, pp 55–60
37. Paridah MT, Juliana AH, Zaidon A, Abdul Khalil HPS (2015) Non-wood-based composites wood structure and function. Curr For Rep 1:221–238
38. Paschoal G, Muller CM, Carvalho GM, Tischer CA, Mali S (2015) Isolation and characterization of nanofibrillated cellulose from oat hulls. Quim Nova 38:478–482
39. Poletto M, Pistor V, Zeni M, Zattera AJ (2011) Crystalline properties and decomposition kinetics of cellulose fibers in wood pulp obtained by two pulping process. Polym Degrad Stab 96:679–685

40. Poletto M, Zattera AJ, Forte MM, Santana RM (2012) Thermal decomposition of wood: influence of wood components and cellulose crystallite size. Bioresour Technol 109:148–153
41. Purohit V, Orzel RA (1988) Polypropylene: a literature review of the thermal decomposition products and toxicity. Int J Toxicol 7:221–242
42. Qadir MI, Abbas K, Hamayun R, Ali M (2014) Analgesic, anti-inflammatory and anti-pyretic activities of aqueous ethanolic extract of *Tamarix aphylla* L. (Saltcedar) in mice. Pak J Pharm Sci 27:1985–1988
43. Rashid U, Anwar F, Knothe G (2011) Biodiesel from milo (*Thespesia populnea* L.) seed oil. Biomass Bioenergy 35:4034–4039
44. Rashid U, Anwar F, Yunus R, Al-Muhtaseb AH (2014) Transesterification for biodiesel production using *Thespesia populnea* seed oil: an optimization study. Int J Green Energy 12:479–484
45. Reddy KO, Ashok B, Reddy KRN, Feng YE, Zhang J, Rajulu AV (2014) Extraction and characterization of novel lignocellulosic fibers from *Thespesia lampas* plant. Int J Poly Anal Charact 19:48–61
46. Rezende CA, de Lima MA, Maziero P, deAzevedo ER, Garcia W, Polikarpov I (2011) Chemical and morphological characterization of sugarcane bagasse submitted to a delignification process for enhanced enzymatic digestibility. Biotechnol Biofuels 4:54
47. Sahari J, Sapuan SM, Zainudin ES, Maleque MA (2013) Mechanical and thermal properties of environmentally friendly composites derived from sugar palm tree. Mater Design 49:285–289
48. Sathyanarayana T, Sarita T, Balaji M, Ramesh A, Boini MK (2004) Antihyperglycemic and hypoglycemic effect of *Thespesia populnea* fruits in normal and alloxan-induced diabetes in rabbits. Saudi Pharm J 12:107–111
49. Schenzel K, St Fischer, Brendler E (2005) New method for determining the degree of cellulose I crystallinity by means of FT Raman spectroscopy. Cellulose 12:223–231
50. Scherrer P (1918) Bestimmung der Gro¨ße und der inneren Struktur von Kolloidteilchen mittels Rontgenstrahlen. Nachrichten Gesells chaft Wissenschaft Gottingen 2:98–100
51. Segal L, Creely JJ, Martin AE Jr, Conrad CM (1962) An empirical method for estimating the degree of crystallinity of native cellulose using the x-ray diffractometer. Textile Res J 29:786–794
52. Siddhanta AK, Prasad K, Meena R, Prasad G, Mehta GK, Chhatbar MU, Oza MD, Kumar S, Sanandiya ND (2009) Profiling of cellulose content in Indian seaweed species. Bioresour Technol 100:6669–6673
53. Solomon A, Beer S, Waisel Y, Jones GP, Paleg LG (1994) Effects of NaCl on the carboxylating activity of Rubisco from *Tamarix jordanis* in the presence and absence of proline-related compatible solutes. Physiol Planta 90:198–204
54. Sun XF, Xu F, Sun RC, Fowler P, Baird MS (2005) Characteristics of degraded cellulose obtained from steam-exploded wheat straw. Carbohydr Res 340:97–106
55. Tesky JL (1992) *Tamarix aphylla*. In: Fire Effects information system. U.S. Department of Agriculture, Forest Service, Forest Products Laboratory, Madison
56. Villegas LF, Fernandez ID, Maldonado H, Torres R, Zavaleta A, Vaisberg AJ, Hammond GB (1997) Evaluation of the wound-healing activity of selected traditional medicinal plants from Peru. J Ethnopharmacol 55:193–200
57.. Whistler RL (1963) Methods in carbohydrate chemistry. Cellulose, vol 3. Academic Press, New York
58. Witter R, Sternberg U, Hesse S, Kondo T, Koch FT, Ulrich AS (2006) C-13 chemical shift constrained crystal structure refinement of cellulose I-alpha and its verification by NMR anisotropy experiments. Macromolecules 39:6125–6132
59. Zahran MA (1982) Ecology of the halophytic vegetation of Egypt. In: Sen DN, Bajpurohit KS (eds) Tasks for vegetation science, vol 2. Dr. W. Junk Publishers, The Hague, pp 3–20
60. Zahran MA, Boulos ST, Kamal El-Din H (1972) Potentialities of fiber plants of Egyptian flora in national economy I. *Juncus rigidus* and paper industry. Bull Inst Deserte Egypte 22:193–203
61. Zahran MA, El-Amier YA (2014) Ecology and establishment of fiber producing taxa naturally growing in the Egyptian deserts. Egypt J Basic Appl Sci 1:104–150
62. Zahran MA, El-Demerdash MA, Mashaly IA (1993) On the ecology of *Juncus acutus* and *J rigidus* as fiber producing halophytes in arid regions. In: Lieth H, Al Masoom AA (eds) Towards the rational use of high salinity tolerant plants tasks for vegetation science, vol 28. Springer, Dordrecht, pp 331–342
63. Zain ME, Awaad AS, Al-Outhman MR, El-Meligy RM (2012) Antimicrobial activities of Saudi Arabian desert plants. Phytopharma 2:106–113
64. Zheng Y, Pan Z, Zhang R, Jenkins BM, Blunk S (2006) Properties of medium-density particleboard from saline Athel wood. Ind Crop Prod 23:318–326
65. Zhou W, Zhu D, Langdon A, Li L, Liao S, Tan L (2009) The structure characterization of cellulose xanthogenate derived from the straw of *Eichhornia crassipes*. Bioresour Technol 100:5366–5369